Sensors and Actuators B 255 (2018) 1753–1761

Contents lists available at ScienceDirect

Sensors and Actuators B: Chemical

journal homepage: www.elsevier.com/locate/snb

Research paper

Enhanced biosensing platform constructed using urchin-like ZnO-Au@CdS microspheres based on the combination of photoelectrochemical and bioetching strategies

Yan Zhao[a], Jian Gong[b], Xiaobin Zhang[a], Rongmei Kong[a], Fengli Qu[a,*]

[a] College of Chemistry and Chemical Engineering, Qufu Normal University, Qufu, Shandong, 273165, PR China
[b] Department of Pharmacy and Biotechnology, Zibo Vocational Institute, Zibo, Shandong, 255314, PR China

ARTICLE INFO

Article history:
Received 10 May 2017
Received in revised form 14 August 2017
Accepted 27 August 2017
Available online 30 August 2017

Keywords:
Urchin-like ZnO microsphere
ZnO-Au@CdS
Photoelectrochemical
Bioetching
H_2O_2 detection
Glucose biosensor

ABSTRACT

Recently, photoelectrochemical (PEC) biosensing has received considerable attention with wide applications in biotechnology and biomedicine. Here we report a novel PEC biosensing platform constructed via the combined strategy of both PEC analysis and bioetching. Urchin-like ZnO-Au@CdS microspheres were obtained by depositing Au nanoparticles (NPs) and CdS NPs on the surface of urchin-like ZnO microspheres. The introduction of intermediate electrotransfer of Au NPs to isolated ZnO and CdS systems significantly enhances the PEC property. CdS NPs can be irreversibly bioetched by an enzymatic reaction catalyzed by horseradish peroxidase (HRP) and H_2O_2. As a result, H_2O_2 detection is realized based on the decrease of the intensity of the PEC signal. This mediator-free and interference-free sensing platform has a linear range from 0.15 to 100 μM with a detection limit of 0.04 μM H_2O_2 at S/N = 3. Furthermore, glucose oxidase (GOD) was successfully immobilized on ZnO-Au@CdS microspheres to construct a glucose biosensor with a detection limit of 0.18 μM at S/N = 3. The PEC biosensor shows good sensing performance with low detection limit, mediator-free and accuracy, strong anti-interference, promising its application in PEC biosensing.

1. Introduction

Photoelectrochemical (PEC) biosensor for rapid and high throughput bioanalysis has attracted considerable research interest in the detection of various biological and biochemical targets such as antigens, nucleic acids, enzymes, enzyme substrates, and chemicals [1–3]. PEC biosensing is a highly sensitive analytical method, because it invovles the use of different forms of energy for excitation (light) and detection (current), which can eliminate undesired background signals [4–6]. An additional benefit of PEC in comparison with other optical detection methods is its simplicity in instrument requirement and low cost inherence for electronic detection (Chen et al., 2010).

The PEC biosensors based on photoactive semiconducting nanomaterials have shown superior performance. In particular, the photoactivity of the semiconductors plays an important role to determine the analytical performance of the PEC biosensors [7,8]. Recently, ZnO has been regarded as a promising photocatalyst owing to its nontoxic and inexpensive characteristics, high thermal and chemical stability, and good electrical and optical properties [9–13]. However, the efficiency of photocurrent conversion of pristine ZnO is still limited because of the relatively optical band gap (ca. 3.37 eV) and high recombination rate of photogenerated electron-hole pairs [4,14]. To solve these problems, ZnO-based semiconductor composites, including TiO_2/ZnO, CuO/ZnO and CdSe/ZnO, have been constructed to improve the photocatalytic activity of ZnO photocatalysts [15–17]. For example, CdS nanoparticles (NPs), with a narrow band gap, have been intensively studied as popular visible light-active materials for PEC biosensor [18,19]. The problem of high recombination rate of photogenerated electrons and holes of pure CdS NPs can be overcome by coupling CdS with ZnO [20]. It is possible to make the charge and hole of ZnO@CdS effectively separated and transferred by a strong interfacial electric field owing to the well-matched overlapping band-structures [21,22]. However, such p-type semiconductors, with cavity as the carrier, have less electrical conductivity than conductive metal. Therefore, rejoining the conductive metal (Au, Pt, Cu et al.) to promote the conductivity property of ZnO@CdS microspheres is necessary [23].

To date, scientific thrust in biosensor is often directed toward the accuracy, stability and sensitivity for constructing mediator-free and interference-free biosensor to achieve practical application.

* Corresponding author.
E-mail address: fengliquhn@hotmail.com (F. Qu).

http://dx.doi.org/10.1016/j.snb.2017.08.191
0925-4005/

The immobilization of redox proteins on a biocompatible electrode surface for biosensing could generally provide a foundation for fabricating the mediator-free biosensor which simplifies the fabrication processes of the sensor and avoids the leaching of the mediator. In addition to the predominance of excellent PEC properties, ZnO-based semiconductor nanostructures have been proved to be a potential electrode material because of their good biocompatibility and relative conductivity, which offers a microenvironment for increasing the quantity and bioactivity of immobilized proteins. On the other hand, the bioetching method is a newly developed and promising analytical method for developing interference-free biosensor. Bioetching is biological manufacturing process, which could occur between redox proteins and material surface. For instance, "3D tissue-etching" technique was developed by successively removing material from a monolithic solid through subtractive manufacturing. Liu et al. reported on the bioetching-based micro-gear used as 3D microstructure system [24,25]. Recently, it was reported that CdS NPs could be catalytically bioetched by an enzyme, horseradish peroxidase (HRP), in the presence of H_2O_2 [24,25]. These successful demonstrations not only have shown the vast allure of this strategy, but also contributed to the constructing interference-free biosensor based on the specifically enzymatic reaction. It would be of great importance and value to develop mediator-free and interference-free biosensing platform using the combination of PEC analysis based on ZnO-CdS semiconductor nanostructures and bioetching strategies.

In recent years, the trace monitoring of small molecules is particularly important, such as the glucose detection in serum for diabetes patients and hydrogen peroxide detection in water samples. Here we report a novel PEC biosensing platform constructed via the combined strategy of both PEC analysis and bioetching method. In particular, ternary urchin-like ZnO-Au@CdS microspheres were obtained by depositing Au NPs and CdS NPs on the surface of ZnO microspheres, where ZnO and CdS served as two isolated PEC parts and Au NPs worked as the electro-transfer part. The introduction of Au NPs between the surface of porous urchin-like ZnO and CdS enhanced the electrical conductivity and PEC property significantly. CdS NPs could be irreversibly bioetched by an enzymatic reaction catalyzed by HRP and H_2O_2, leading to a decrease of the intensity of the PEC property. The use of light as excitation energy and current as detection signal eliminated the undesired background signals, which made the ultra sensitive H_2O_2 detection realized based on the decrease of the intensity of the PEC signal.

A glucose biosensor was constructed by immobilizing glucose oxidase (GOD) on the ZnO-Au@CdS microspheres. The urchin-like ZnO-Au@CdS microspheres had good biocompatibility and big specific surface, which were good electrode material for sufficient and stable immobilization of GOD. The special enzyme-catalyzed bioetching reaction and the use of different forms of energy for excitation and detection contributed to the mediator-free, interference-free and sensitive detection of glucose. The developed glucose biosensor had a linear range of 0.50–400 μM with a detection limit of 0.18 μM at S/N = 3. To the best of our knowledge, it was the first time that the combined strategy of both PEC analysis and bioetching method was proposed and verified in biosensing, which facilitated the detection of H_2O_2 and glucose realized under mild physiological conditions.

2. Experimental section

2.1. Materials and reagents

Zinc acetate dihydrate ($Zn(CH_3COO)_2{\cdot}2H_2O$), hexamethylenetetramine (HMT, $C_6H_{12}N_4$), sodium citrate (Na_3CA), chloroauric acid tetrahydrate ($HAuCl_4{\cdot}4H_2O$), copper(II) perchlorate hexahydrate ($Cd(ClO_4)_2{\cdot}6H_2O$), ascorbic acid (AA), glucose, and HRP (5.0 mg/mL) were purchased from Sinopharm Chemical Reagent Co. LTD. (Shanghai, China). GOD (5.0 mg/mL) was obtained from Sigma-Aldrich Co. LLC. (St. Louis, USA). Sulphur (S8), N-(3-dimethylaminopropyl)-N′-ethyl-carbodiimide hydrochloride (EDC), N-hydroxysuccinimide (NHS) and mercaptopropionic acid (MPA) were purchased from Aladdin Industrial Inc. (Shanghai, China). Graphene oxide (GO) was obtained from Leadernano Tech. L.L.C. (Jining, China). All other reagents were used as received without further purification. All aqueous solutions were prepared with ultrapure water (resistivity >18 MΩ cm) produced using a Millipore system. The glass substrates (ITO) were ultrasonically cleaned with ethanol, acetone and deionized water before use.

2.2. Apparatus

The morphology and structure of the obtained products were characterized by a field emission scanning electron microscopy (SEM) JSM-6700F microscope and a high-resolution transmission electron microscopy (HRTEM) JEM-2100 microscope, respectively. The crystallinity and phase of the products were determined by an X-ray diffraction (XRD) MiniFlex600 (Rjgaku Co. Japan) diffractometer. X-ray photoelectron spectroscopy (XPS) analysis was conducted on an ESCALAB 250Xi spectrometer (Thermo Fisher, USA). After pretreatment, nitrogen adsorption and desorption isotherma were measured at 77 K on a Quantachrome Instrument NOVA. PEC measurements were performed with an assembled PEC system. A 300W Xe lamp was used as the irradiation source with a light intensity of 300 $\mu W\,cm^{-2}$ estimated by a radiometer (Ceaulight Corporation, China). Photocurrent was measured on a CHI760D electrochemical workstation (Shanghai Chenhua Apparatus Corporation, China) with a three-electrode system. A modified ITO electrode with a geometrical area of $1.0 \pm 0.1\,cm^2$ was the working electrode, a Pt wire was the counter electrode, and a saturated Ag/AgCl electrode was the reference electrode.

2.3. Synthesis of urchin-like ZnO and ZnO-Au

The urchin-like ZnO microsphere was synthesized according to the method reported in the literature with necessary modifications [26]. In a typical procedure, 0.1 M of $Zn(CH_3COO)_2{\cdot}2H_2O$, 0.1 M of HMT and 0.01 M of sodium citrate were contained in 10 mL of distilled water. The mixed solution was heated at 90 °C for 4 h. After the reaction, a white product was obtained and would be washed with ultrapure water for several times. Finally, the product was annealed at 400 °C for 30 min and cooled down naturally.

20 mg of the as-prepared urchin-like ZnO microspheres was dispersed in 100 mL of ultrapure water and mixed with 0.544 mL of $HAuCl_4{\cdot}4H_2O$ (1 wt%) solution under stirring. The mixed solution was heated at 110 °C after stirring for 15 min. 3 mL of Na_3CA (0.04 M) solution was added into the reaction solution to reduce $HAuCl_4$ and form metallic Au NPs. After stirring for approximately 40 min, a pink precipitate was obtained, followed by centrifugation. The color change from white to pink suggested the successful formation and decoration of Au NPs on the ZnO microspheres.

2.4. Synthesis of ZnO-Au@CdS

20 mg of the as-prepared ZnO-Au was introduced to an ethanol suspension with a volume of 50 mL containing 2.0 mM of S8 and 4.0 mM of $Cd(ClO_4)_2{\cdot}6H_2O$. The suspension was irradiated under a Xe lamp (500 W) for 7 h. After centrifugation and washing with ethanol for several times, the resulting ZnO-Au@CdS microspheres were dried in an oven at 80 °C for 6 h.

2.5. Preparation of the ITO/GO/ZnO-Au@CdS electrode

The ITO electrodes were washed by acetone, ethanol/NaOH mixed solution (v/v, 1:1) and water respectively, followed by drying at 60 °C for 2 h. The ITO electrode was modified with GO (ITO/GO) by drop-coating 30 μL of GO solution (1.0 mg/mL). The ultrathin transparent GO nanosheet was used to immobilize ZnO-Au@CdS for the fabrication of the biosensor, which exhibited high benefit in accelerating the electron transfer. Before the GO dried, 30 μL of ZnO-Au@CdS (0.8 mg/mL) solution was dropped onto the electrode surface to construct the ITO/GO/ZnO-Au@CdS electrode. In the same way, the ITO/GO/ZnO, ITO/GO/ZnO-Au and ITO/GO/ZnO@CdS electrode were constructed for the control experiments.

2.6. Preparation of the ITO/GO/ZnO-Au@CdS glucose biosensor

The ITO/GO/ZnO-Au@CdS electrode was immersed into 0.1 M of PBS buffer (pH 7.4, containing 3 mM MPA) for 5 h at 4 °C. After that, the electrode was immersed into a solution containing 0.1 M of EDC and NHS for 2 h at 4 °C and was washed with PBS buffer for several times to remove unreacted molecules. Under humid conditions, 30 μL of PBS buffer containing 5.0 mg/mL of HRP was added onto the modified electrode to construct ZnO-Au@CdS based H_2O_2 biosensor. After incubation at 4 °C for 2 h, the electrode was rinsed with PBS buffer and stored at 4 °C for further use. In the same way, 5.0 mg/mL GOD was further co-immobilized on the ITO/GO/ZnO-Au@CdS electrode to construct glucose biosensor.

2.7. PEC measurements

PBS buffer solution containing various concentrations of H_2O_2, 5 mM of NaBr and 0.1 M of AA with a final volume of 20 mL was used as test solution. AA was served as a sacrificial electron donor during the photocurrent measurement. The modified electrode was immersed into the test solution for 5 min for the bioetching of CdS, and the PEC detection was carried out at room temperature. The Xe lamp with a spectral range of 200–2500 nm was utilized to produce white light as an excitation light, which was switched on and off every 20 s with the applied potential of −0.2 V.

3. Results and discussions

3.1. Principle of PEC-bioetching assay based on urchin-like znO-Au@CdS microspheres

The electron mediators of electrode surface-modified could control the electrochemical reaction rate at the electrode surface to achieve selective electrocatalytic effects. As an excellent electrode modification material, GO has excellent structural properties and electrocatalytic performance. In this experimental system, GO is not only one of the materials for the construction of the ITO/GO/ZnO-Au@CdS electrode to immobilize ZnO-Au@CdS, but also accelerates the efficiency of electron transfer.

Both Au NPs and CdS NPs were selectively deposited on the polar surfaces of ZnO crystals to construct urchin-like ZnO-Au@CdS microspheres with good electrical conductivity and PEC property. The modification of Au NPs could significantly enhance the light absorption and facilitate the separation and transport of photogenerated carriers through the effect of localized surface plasmon resonance (LSPR) [27]. The schematic of the photocatalyst mechanism of the composites was given in Scheme 1A. The position of CdS and ZnO bands had type-II alignment where the conduction band edge of ZnO was located between the conduction band and the valence band of CdS. In this configuration, when the electron–hole pairs were generated by visible-light excitation in CdS NPs (shell), the photoelectrons could be transferred to the conduction band of ZnO, which facilitated the process of charge separation process of the electron–hole pairs before they recombined. In addition, the Au NPs induced LSPR and surface potential at ZnO@CdS interface together facilitated rapid carrier separation and transport. Thus, the photocorrosion induced by oxidation could be effectively dampened by the rapid reaction rate. According to previous report, a facial, fast and straightforward bioetching process of CdS NPs could be enzymatically catalyzed by HRP in the presence of H_2O_2. After the bioetching of CdS NPs, a slight photocurrent conversion efficiency could be produced (Scheme 1B) because the ZnO-Au microspheres could only harvest ultraviolet light.

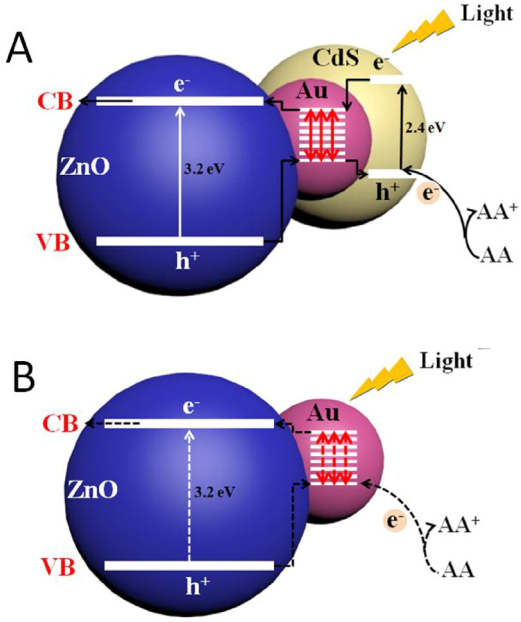

Scheme1. Schematic of the charge-carrier transfer process in (A) the ZnO-Au@CdS microsphere and (B) ZnO-Au microsphere.

The enzymatic etching process of CdS NPs by HRP in the presence of H_2O_2 was shown in Scheme 2A. HRP could catalyze the oxidation of S^{2-} ions in CdS NPs in the presence of H_2O_2, resulting in the formation of sulfate anions and Cd^{2+} cations [28]. The driving force of the bioetching process was biocatalytic oxidation of S^{2-} yielding $SO_4{}^{2-}$ ions according to Eqs. (1) and (2):

$$CdS \rightarrow Cd^{2+} + S^{2-} \quad (1)$$

$$S^{2-} + H_2O_2 \rightarrow SO_4{}^{2-} + H_2O[29] \quad (2)$$

As illustrated in Scheme 2B, an ultrasensitive PEC sensing platform for H_2O_2 and glucose detection was developed based on bioetching process. A cascade reaction occurred in the presence of dissolved oxygen. The first reaction was the conversion of glucose by GOD into gluconic acid and H_2O_2. The bioetching of semiconductor of CdS NPs by H_2O_2 in the presence of HRP and NaBr led to a decrease of the photocurrent intensity. As a comparison, there was no significant change of the photocurrent in the absence of HRP or H_2O_2. The detailed reaction mechanism was presented below:

$$Glucose + GOD_{(FAD)} \rightarrow gluconicacid + GOD_{(FADH2)} \quad (3)$$

$$GOD_{(FADH2)} + O_2 \rightarrow GOD_{(FAD)} + H_2O_2 \quad (4)$$

$$HRP(red) + H_2O_2 \rightarrow HRP(ox) + H_2O \quad (5)$$

$$HRP(ox) + S^{2-} \rightarrow HRP(red) + SO_4{}^{2-} \quad (6)$$

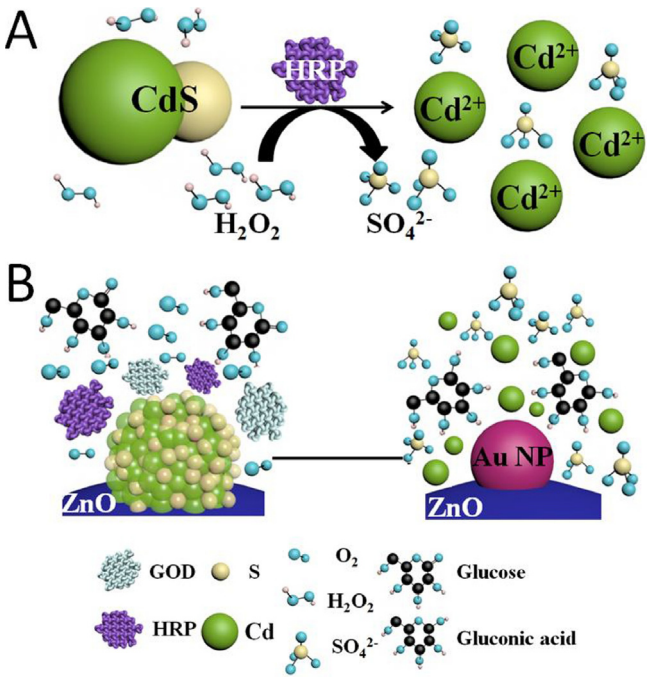

Scheme 2. Schematic illustration of (A) enzymatic bioetching of CdS NPs and (B) enzymatic bioetching process of the ZnO-Au@CdS biosensor.

3.2. Morphology and spectroscopic characterizations

The morphology of the as-prepared ZnO and ZnO-Au was observed by SEM measurements. The low-magnification SEM image showed that uniform urchin-like ZnO microspheres with a diameter of 3–4 μm were successfully synthesized (Fig. 1A). The self-assembled nanoplates of the ZnO microspheres had a thickness of tens of nanometers and the separation between two adjacent nanoplates was approximately several hundreds nanometers. The N_2 adsorption/desorption isotherms of the sample was shown in Fig. S1 and the Brunauer-Emmett-Teller (BET) surface areas were measured to be 40.86 m^2/g, which was better than that of many other ZnO based nanostructures and was promising for biosensors and hydrogenation catalysts [30]. Fig. 1B displayed a SEM image of ZnO microspheres decorated with Au NPs, which were several tens nanometers and uniformly distributed on the surface of ZnO microspheres. The HRTEM image and selected area electron diffraction (SAED) pattern of ZnO-Au@CdS microspheres were given in Fig. 1C. Uniform CdS NPs with a size of 4 nm were deposited on the surface of ZnO-Au microsphere. The measured spacing of the crystallographic plane was 0.335 nm, which could be indexed to the {111} lattice plane of a hexagonal CdS crystal [31]. No buffer layers, crystalline or amorphous part were observed in the interface regions. The EDX spectrum taken from the surface of a ZnO-Au and ZnO-Au@CdS microspheres were presented in Fig. 1D, which confirmed the elemental presence of Zn, O, Cd, and S in the product. The peaks of C and Cu were originated from the Cu grid during TEM measurements. The peaks of Zn, O and Au were recorded for ZnO-Au and the rest of peaks of Cd and S were attributed to ZnO-Au@CdS. The atomic percentage of Au in ZnO-Au and ZnO-Au@CdS was 10.35% and 4.52%, respectively. The morphologies of ZnO-Au were unchanged after etching from the SEM analysis (Fig. S2A), while the atomic percentage of Cd decreased from 11.29% to 0.40% after CdS NPs were bioetched (Fig. S2B).

The urchin-like ZnO microspheres, ZnO-Au, ZnO-Au@CdS microspheres and ZnO-Au after bioetching were identified by XRD (Fig. 2A). For the ZnO microspheres, the main reflection peaks matched with the standard data of the wurtzite structure of ZnO (JCPD card no. 36-1451) [32]. And, there was no extra peak detected by XRD, which confirmed the superior purity of the ZnO microspheres. For the ZnO-Au microspheres, an extra weak peak at 38.1° could be indexed to {111} lattice plane of Au. For the ZnO-Au@CdS microspheres, new diffraction peaks were indexed to the wurtzite CdS phase (JCPDS Card no. 65-3414). After the bioetching procedure, crystal CdS were expended gradually, no specific diffraction peaks of CdS could be found.

The full range XPS spectra further confirmed the surface compositions and elemental analysis of ZnO-Au@CdS (Fig. 2B). The peaks located at 1044.94, 531.69, 87.39, 411.79 and 162.24 eV were attributed to Zn, O, Au, Cd and S in the ZnO-Au@CdS microspheres, respectively. In the expanded XPS spectra, Fig. 2C presented the XPS spectrum of Zn 2p. The peak position of Zn 2p1/2 and Zn 2p3/2 was located at 1044.94 and 1021.84 eV, respectively. The high resolution O 1s and O-Zn group spectra of Fig. 2D showed specific peaks centered at 531.69 and 530.34 eV, respectively. The high resolution XPS spectra of Au 4f and Zn 3p were shown in Fig. 2E. Two significant binding energy peaks at 87.39 and 83.58 eV were corresponded to the electronic states of Au 4f5/2 and Au 4f7/2, respectively. These results suggested that Au was present in the zero-valent state, indicating the formation of Au NPs on the ZnO microsphere. Two interference peaks (91.19 and 88.24 eV) attributed to Zn 3p also presented along with Au 4f peaks as shown in Fig. 2E. The spectrum of Cd 3d in Fig. 2F was subdivided into two separated peaks that correspond to Cd 3d3/2 (411.79 eV) and Cd 3d3/2(405.09 eV) valence states. The spectrum of S 2p at 162.24 eV showed that the CdS NPs were well synthesized (Fig. 2G). Therefore, XPS analysis confirmed the presence of Au, CdS, and ZnO in the resultant product, which was in accordance with the results of XRD analysis.

3.3. PEC property of ZnO-Au@CdS electrode

As shown in Fig. 3A, the photocurrent response of as-prepared bioassay was tested. As ZnO could only harvest ultraviolet light and lead to low efficiency of photocurrent conversion, the ITO/GO/ZnO electrode exhibited a small intensity of photocurrent (curve a, I = 8.3 μA). The ITO/GO/ZnO-Au electrode had a litter higher current intensity (curve b, I = 8.9 μA) because Au NPs could enhance the electron transfer. After ZnO-Au@CdS was deposited on the electrode, the photocurrent intensity (curve c, I = 105.3 μA) increased to 12.7 times higher than that of ITO-GO-ZnO electrode. This was attributed to the large surface area of GO and the extension of the absorb range to middle-wavelength light (500 nm to 600 nm). Furthermore, the doped Au NPs significantly inhibited the electro-hole recombination. After the bioetching process, the intensity of photocurrent decreased (curve d, I = 78.6 μA) as CdS amount decreased.

As shown in Fig. 3B, ITO/GO/ZnO-Au@CdS electrode was easier to achieve a smooth current value compared with ITO/GO/ZnO@CdS electrode. A transition time was needed in ITO/GO/ZnO@CdS electrode because the electronics between semiconductors could not fully transmitted. The effect of the bioetching time on the response of the PEC biosensor was presented in Fig. 3C. The photocurrent leveled off after 3 min and reached equilibrium after 5 min. Consequently, 5 min was selected as the optimized detection time for the PEC biosensor.

3.4. Optimization for the fabrication of the H_2O_2 and glucose assay

The detection conditions were optimized for PEC determination. The photocurrent increased as the volume of GO (V_{GO}) increased from 0 to 30 μL (Fig. S3A). A maximum photocurrent was observed with a volume of 30 μL and then decreased with additional GO.

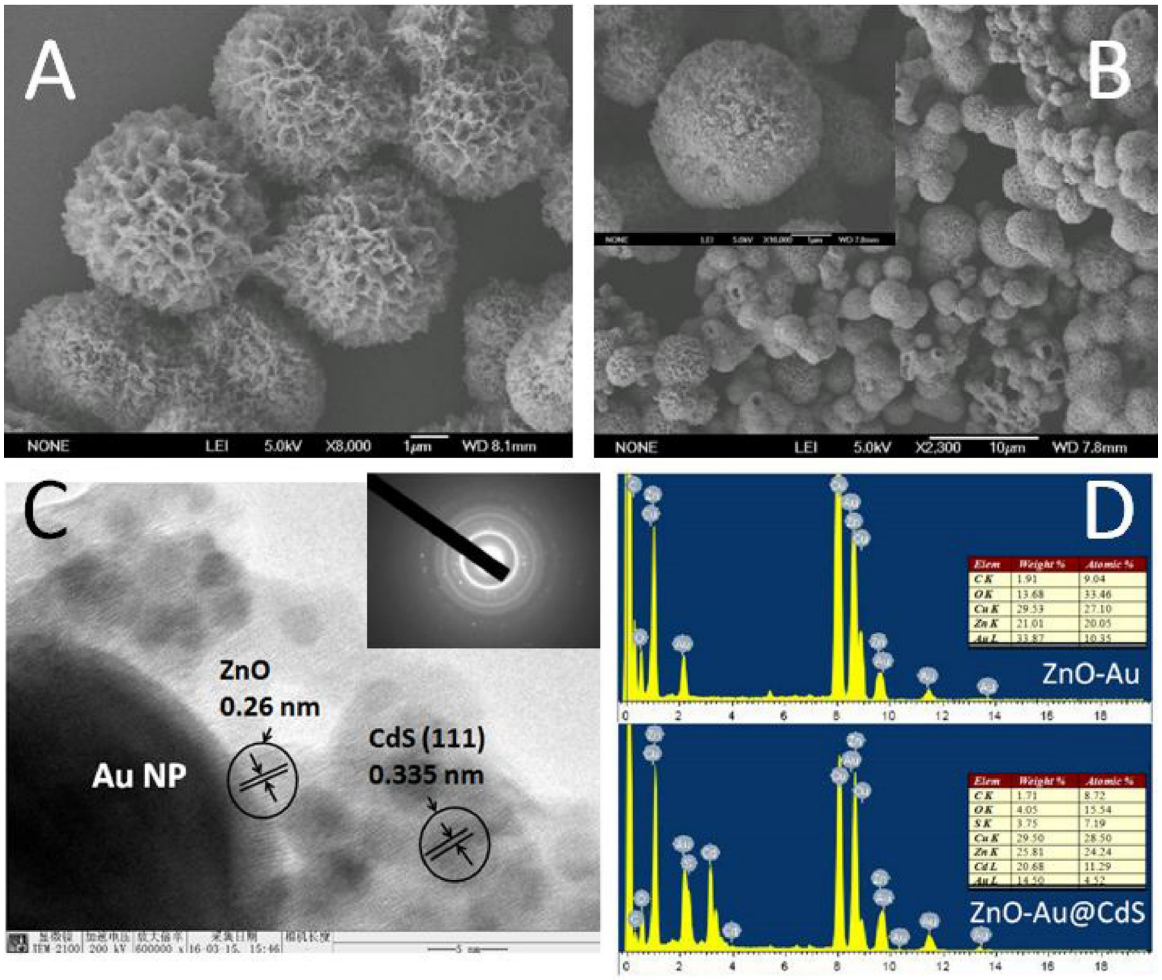

Fig. 1. SEM images of (A)ZnO, (B) ZnO-Au and the magnified ZnO-Au (inset), (C) HRTEM image of ZnO-Au@CdS and the corresponding SAED image (inset), and (D) EDS spectra of ZnO-Au and ZnO-Au@CdS and the corresponding elements contents.

The excessive GO on the electrode might inhibit electron and proton transport. Therefore, 30 μL of GO solution was selected as the optimal volume for the deposition.

CdS NPs could be bioetched to Cd^{2+} by HRP in the presence of H_2O_2, and glucose could be oxidized to gluconic acid and H_2O_2 by GOD in the dissolved oxygen solution. Since HRP and GOD played different roles, the ratio of two enzymes determined the performance of the biosensor. The volume ratio (from 0:1 to 1:0 with a total volume of 30 μL) of bienzyme (HRP/GOD) was examined under Xe lamp irradiation when the concentration of glucose was set at 100 μM (Fig. S3B). With the increased amount of GOD, the cascade reaction was triggered and the catalytic activity steadily increased. Lower catalytic activity was observed with excessive GOD and the possible reason was local overproduction of H_2O_2 by GOD rapidly saturated and inhibited the enzymatic activity of HRP. The volume ratio of 2:1 for HRP/GOD yielded the highest catalytic ability and was used in the further experiments.

Furthermore, the contents of enzymes (HRP and GOD) were investigated to obtain an optimal PEC response for the system (Fig. S3C). The photocurrent decreased with the increasing volume of enzymes. The PEC response achieved a terrace in the presence of 30 μL of total volume of enzyme and fluctuated slightly thereafter, which could attribute to the balance of the steric hindrance and the electron transfer of enzymes [33,34].

3.5. Analytical performance of the PEC biosensor

After optimization for the fabrication of the H_2O_2 assay, the detection of H_2O_2 with high sensitivity based on the ZnO-Au@CdS microspheres was achieved. As the concentration of H_2O_2 increased, the photocurrent intensity decreased resulted from the bioetching of CdS NPs (Fig. 4A). Good correlation between the concentration of H_2O_2 and the current intensity was observed with a wide dynamic range from 0.15 to 100 μM (Fig. 4A, inset). The linear regression equation was $A = -1.03C + 103.00$ ($R^2 = 0.996$), where A (μA) was the photocurrent response and C (μM) was the concentration of H_2O_2. 3× standard deviation of the blank signal/sensitivity was chosen as the limit of detection (LOD), while the blank analyte still produced signal response, and the LOD concentration was 0.04 μM at S/N = 3.

The ZnO-Au@CdS was used to develop glucose biosensor due to the high sensitivity detection of H_2O_2. As indicated in Fig. 4B, the ITO/GO/ZnO-Au@CdS electrode exhibited linearity for the concentration of glucose with a linear regression equation of $A = -0.25C + 100.31$ ($R^2 = 0.992$), and a LOD concentration of 0.18 μM at S/N = 3 was achieved. In the meantime, there existed a signal draft for the recorded glucose/H_2O_2 photocurrent. Not all of the H_2O_2 participated the cascade reaction between H_2O_2 and glucose, as part of them participated the oxidation of S^{2-} ions in the formation of sulfate anions, leading the various detection

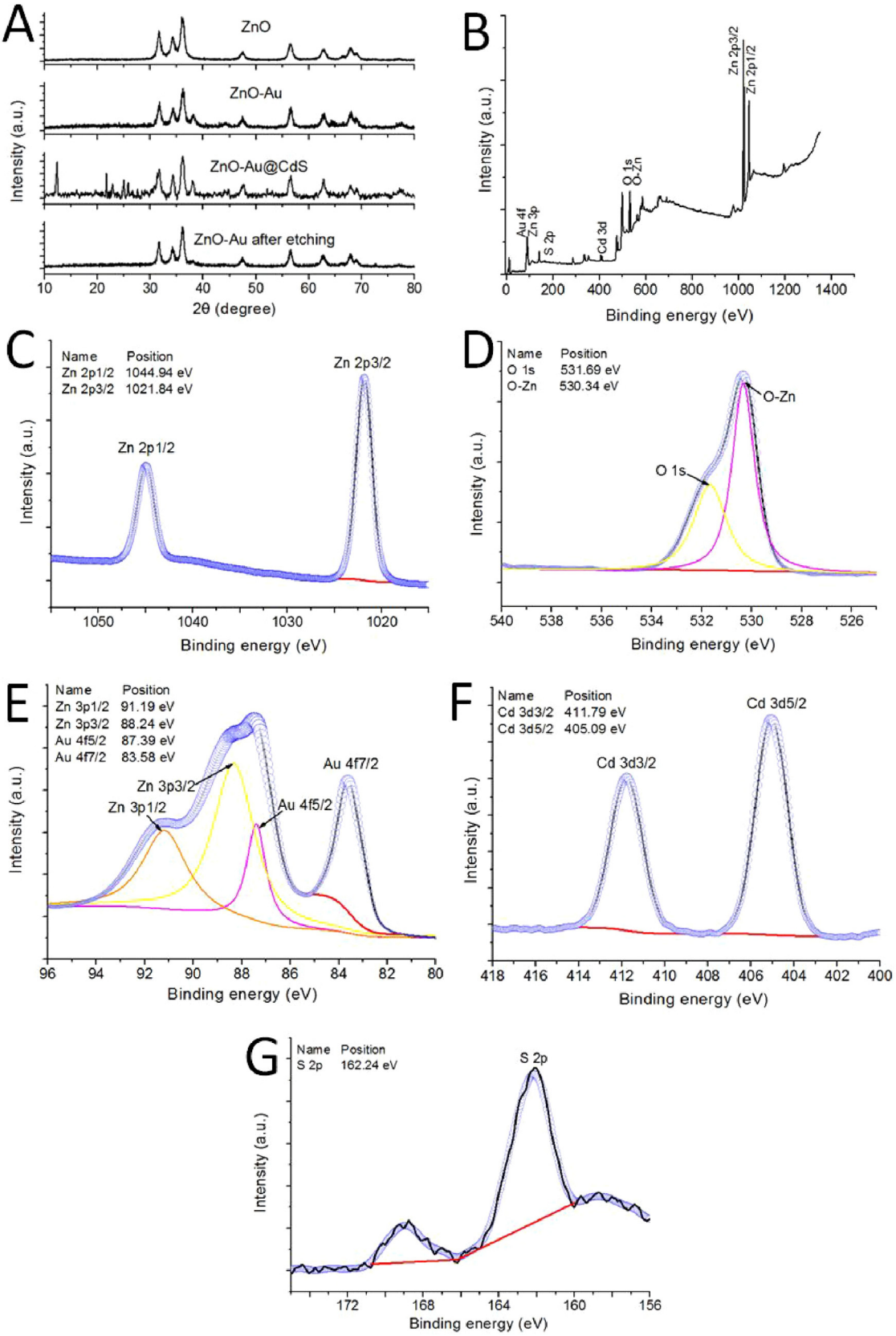

Fig. 2. (A) XRD of ZnO, ZnO-Au, ZnO-Au@CdS and ZnO-Au@CdS after bioetching. (B) Survey XPS spectrum of ZnO-Au@CdS, and (C-G) the high-resolution element spectrum.

range of glucose and H_2O_2. Compared to a smooth photocurrent change for the detection of H_2O_2, the lines had larger fluctuations for the detection of glucose. This might be attributed to the addition of GOD increased the steric hindrance, which resulted in the electronic accumulation and the electron flow was inhibited during the cascade enzymatic reaction. The good performance

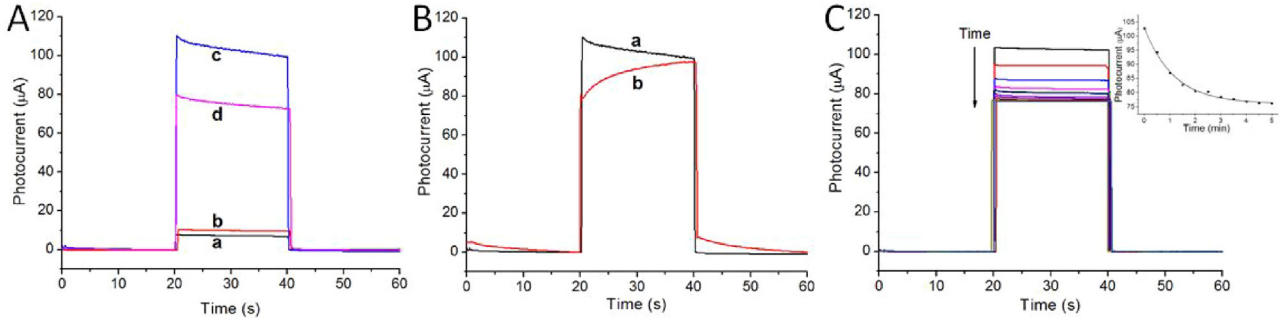

Fig. 3. (A) Photocurrent responses of the (a) ITO/GO/ZnO, (b) ITO/GO/ZnO-Au, (c) ITO/GO/ZnO-Au@CdS and (d) ITO/GO/ZnO-Au@CdS after bioetching. (B) Photocurrent responses of the (a) ITO/GO/ZnO-Au@CdS, (b) ITO/GO/ZnO@CdS. (C) The effect of bioetching time using 20 μM of H_2O_2.

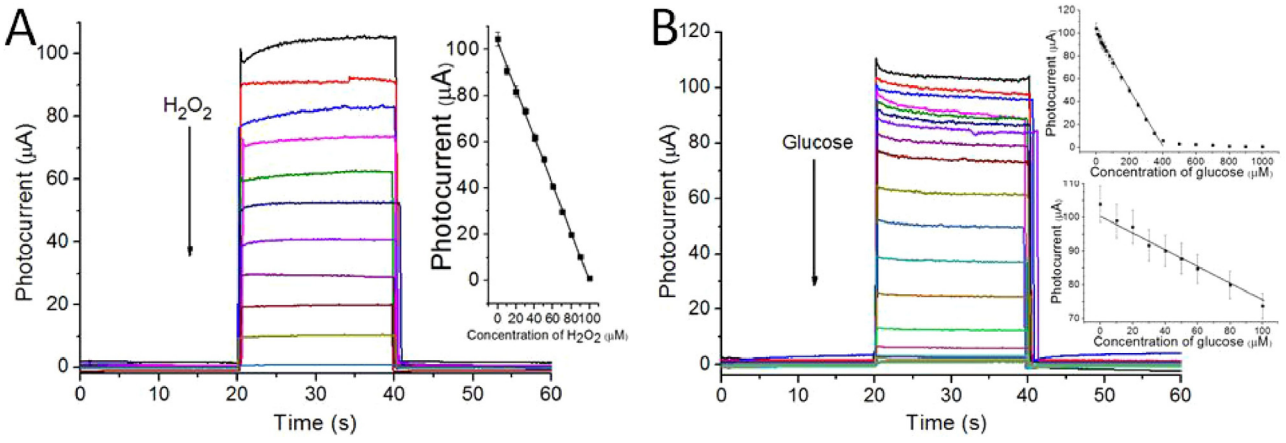

Fig. 4. Photocurrent response of the biosensor for the detection of different concentrations of (A) H_2O_2 from 0 μM to 100 μM and (B) glucose from 0 μM to 1000 μM. The inset figures show the calibration curve with error bars with the standard deviation of three replicate determinations.

of the developed ITO/GO/ZnO-Au@CdS photo-electrochemical glucose biosensor was compared with the reported literatures in Table S1-1 and similar modification methods in Tables S1 and S2.

3.6. Selectivity and reproducibility of the biosensor

The determination of glucose was of great importance for the food and pharmaceutical industry as well as for clinical testing [35,36]. Good specificity for glucose was necessary for a new designed sensing system with potential applications in real samples [37,38]. To evaluate the specificity of the developed signal amplified bioassay for glucose, several potential interfering compounds were studied under the same conditions. The glucose solution (400 μM) containing 4 mM interferences including carbohydrates, cancer biomarkers and ions were measured using the developed bioassay. As shown in Fig. S4, the mixed compound caused a dramatic decrease of photocurrent while these potential interferences triggered negligible signal. The interferences could be negligible since GOD was highly specific for glucose, indicating that the selectivity of the bioassay was quite acceptable and the interferences of a common component could be neglectable for the detection of glucose.

In probable theory and statistics, the coefficient of variation is a standardized measure of dispersion of a probability distribution or frequency distribution. The coefficients of variation were determined by measuring samples with the same concentrations using five electrodes prepared independently under identical experimental conditions. The coefficients of variation for intra-assay runs of H_2O_2 (50 μM) and glucose (100 μM) were 3.7% and 6.2%, respectively, whereas the inter-assay coefficients of variation were 6.9% and 9.4%, respectively. These results suggested that the PEC biosensor exhibited excellent reproducibility in both precision and fabrication.

3.7. Analysis of real samples

Vigorous treatment of foods with hydrogen peroxide may cause some destruction of ascorbic ooooacid, methionine, and cystine [39]. Insufficient data are available to ensure a lack of hazard with water or when more rigorous treatments are employed, using higher concentrations, prolonged exposure, or elevated temperatures. So it is particularly important to make sure the water have no or only trace amounts of hydrogen peroxide. ZnO-Au@CdS microspheres were applied for the analysis of real tap water samples for the recovery response of this system. The real tap water samples were collected in Qufu, China and spiked with different concentrations of H_2O_2. The recovery of this system (Table S2) was close to 100%, indicating that the enzymatic bioetching was suitable for the detection of H_2O_2 in real samples.

In order to evaluate the potential application of the bioassay in complex biological samples, the glucose detection was also conducted in human serum samples. Because blood sugar levels were located in millimole level, three diluted human serum samples (0.1%) were performed for the detection of glucose using the standard addition method. As shown in Table S3, 10 μM, 50 μM, and 100 μM of glucose were added into the diluted serum samples, respectively. The recovery percentage of glucose ranged from 94.5% to 116.8%, and the relative standard deviation (RSD) ranged from

0.9% to 6.1%. These results revealed that the proposed bioassay could be applicable for the practical detection of glucose in real biological samples with other potential interferences.

4. Conclusion

In summary, a novel biosening platform was constructed using both PEC biosensing and bioetching strategy, which was based on the fact that CdS NPs could be irreversibly bioetched by an enzymatic reaction catalyzed by HRP and H_2O_2. The morphology and composition of the synthesized ZnO-Au@CdS were well characterized by SEM, HRTEM, XRD and XPS and the as-prepared biosening platform had excellent performances such as remarkably stability, high sensitivity, mediator free and interference free properties. The sensing platform was successfully applied for the sensitive detection of H_2O_2 and glucose in tap water samples and human serum samples with satisfactory results. The strategy of combined PEC analysis and bioetching opened up a new path for the sensitive detection of H_2O_2 and glucose, which had potential application in the field of biotechnology, biomedical and environmental chemistry.

Acknowledgement

This work was supported by the National Natural Science Foundation of China (21775089, 21375076), the Key Research and Development Program of Shandong Province (2015GSF121031)and the Project of University-industry Cooperation of Jining City (2014018).

Appendix A. Supplementary data

Supplementary data associated with this article can be found, in the online version, at http://dx.doi.org/10.1016/j.snb.2017.08.191.

References

[1] X. Zeng, W. Tu, J. Li, J. Bao, Z. Dai, Photoelectrochemical biosensor using enzyme-catalyzed in situ propagation of CdS quantum dots on graphene oxide, ACS Appl. Mater. Interfaces 6 (2014) 16197–16203.
[2] Z.Y. Ma, Y.F. Ruan, N. Zhang, W.W. Zhao, J.J. Xu, H.Y. Chen, A new visible-light-driven photoelectrochemical biosensor for probing DNA-protein interactions, Chem. Commun. 51 (2015) 8381–8384.
[3] C. Li, H. Wang, J. Shen, B. Tang, Cyclometalated iridium complex-based label-free photoelectrochemical biosensor for DNA detection by hybridization chain reaction amplification, Anal. Chem. 87 (2015) 4283–4291.
[4] S.A. Ansari, M.M. Khan, S. Kalathil, A. Nisar, J. Lee, M.H. Cho, Oxygen vacancy induced band gap narrowing of ZnO nanostructures by an electrochemically active biofilm, Nanoscale 5 (2013) 9238–9246.
[5] H. Wang, Y. Bai, Q. Wu, W. Zhou, H. Zhang, J. Li, et al., Rutile TiO2 nano-branched arrays on FTO for dye-sensitized solar cells, Phys Chem. Chem. Phys. 13 (2011) 7008–7013.
[6] R.M. Kong, Y. Zhao, Y. Zheng, F.L. Qu, Facile synthesis of ZnO/CdS@ZIF-8 core–shell nanocomposites and their applications in photocatalytic degradation of organic dyes, RSC Adv. 7 (2017) 31365–31371.
[7] W.W. Zhan, Q. Kuang, J.Z. Zhou, X.J. Kong, Z.X. Xie, L.S. Zheng, Semiconductor@metal–organic framework core–shell heterostructures: a case of ZnO@ZIF-8 nanorods with selective photoelectrochemical response, J. Am. Chem. Soc. 135 (2013) 1926–1933.
[8] T. Hisatomi, J. Kubota, K. Domen, Recent advances in semiconductors for photocatalytic and photoelectrochemical water splitting, Chem. Soc. Rev. 43 (2014) 7520–7535.
[9] A. Kargar, Y. Jing, S.J. Kim, C.T. Riley, X. Pan, D. Wang, ZnO/CuO heterojunction branched nanowires for photoelectrochemical hydrogen generation, ACS Nano 7 (2013) 11112–11120.
[10] M. Shao, F. Ning, M. Wei, D.G. Evans, X. Duan, Hierarchical nanowire arrays based on ZnO core-layered double hydroxide shell for largely enhanced photoelectrochemical water splitting, Adv. Funct. Mater. 24 (2014) 580–586.
[11] J. Wang, P. Yang, X. Wei, High-performance, room-temperature, and no-humidity-impact ammonia sensor based on heterogeneous nickel oxide and zinc oxide nanocrystals, ACS Appl. Mater. Interfaces 7 (2015) 3816–3824.
[12] D.I. Son, B.W. Kwon, D.H. Park, W.S. Seo, Y. Yi, B. Angadi, et al., Emissive ZnO-graphene quantum dots for white-light-emitting diodes, Nat. Nano 7 (2012) 465–471.
[13] D. Bi, G. Boschloo, S. Schwarzmuller, L. Yang, E.M.J. Johansson, A. Hagfeldt, Efficient and stable CH3NH3PbI3-sensitized ZnO nanorod array solid-state solar cells, Nanoscale 5 (2013) 11686–11691.
[14] R.C. Pawar, C.S. Lee, Single-step sensitization of reduced graphene oxide sheets and CdS nanoparticles on ZnO nanorods as visible-light photocatalysts, Appl. Catal. B 144 (2014) 57–65.
[15] R. Fateh, R. Dillert, D. Bahnemann, Self-cleaning properties, mechanical stability, and adhesion strength of transparent photocatalytic TiO2-ZnO coatings on polycarbonate, ACS Appl. Mater. Interfaces 6 (2014) 2270–2278.
[16] X. Tu, S. Luo, G. Chen, J. Li, One-pot synthesis, characterization, and enhanced photocatalytic activity of a BiOBr-graphene composite, Chem.-A Eur. J. 18 (2012) 14359–14366.
[17] C. Eley, T. Li, F. Liao, S.M. Fairclough, J.M. Smith, G. Smith, et al., Nanojunction-mediated photocatalytic enhancement in heterostructured CdS/ZnO, CdSe/ZnO, and CdTe/ZnO nanocrystals, Angew. Chem. Int. Ed. 53 (2014) 7838–7842.
[18] J. Yu, J. Jin, B. Cheng, M. Jaroniec, A noble metal-free reduced graphene oxide-CdS nanorod composite for the enhanced visible-light photocatalytic reduction of CO2 to solar fuel, J. Mater. Chem. A 2 (2014) 3407–3416.
[19] O. Chen, J. Zhao, V.P. Chauhan, J. Cui, C. Wong, D.K. Harris, et al., Compact high-quality CdSe–CdS core–shell nanocrystals with narrow emission linewidths and suppressed blinking, Nat. Mater. 12 (2013) 445–451.
[20] Y. Hu, X. Gao, L. Yu, Y. Wang, J. Ning, S. Xu, et al., Carbon-coated cds petalous nanostructures with enhanced photostability and photocatalytic activity, Angew. Chem. 125 (2013) 5746–5749.
[21] G. Yang, W. Yan, Q. Zhang, S. Shen, S. Ding, One-dimensional CdS/ZnO core/shell nanofibers via single-spinneret electrospinning: tunable morphology and efficient photocatalytic hydrogen production, Nanoscale 5 (2013) 12432–12439.
[22] S.R. Lingampalli, U.K. Gautam, C.N.R. Rao, Highly efficient photocatalytic hydrogen generation by solution-processed ZnO/Pt/CdS, ZnO/Pt/Cd1-xZnxS and ZnO/Pt/CdS1-xSex hybrid nanostructures, Energy Environ. Sci. 6 (2013) 3589–3594.
[23] F. Xu, Y. Yuan, H. Han, D. Wu, Z. Gao, K. Jiang, Synthesis of ZnO/CdS hierarchical heterostructure with enhanced photocatalytic efficiency under nature sunlight, CrystEngComm 14 (2012) 3615–3622.
[24] Y. Liu, W. Shi, Y. Zhang, X. Wang, Analysis on qualities of bio-etching processing micro-gear part, International Conference on Mechanic Automation and Control Engineering (2010) 5792–5794.
[25] M. Hazar, Y.T. Kim, J. Song, P.R. LeDuc, L.A. Davidson, W.C. Messner, 3D bio-etching of a complex composite-like embryonic tissue, Lab Chip 15 (2015) 3293–3299.
[26] W. Xia, C. Mei, X. Zeng, G. Fan, J. Lu, X. Meng, et al., Nanoplate-built ZnO hollow microspheres decorated with gold nanoparticles and their enhanced photocatalytic and gas-sensing properties, ACS Appl. Mater. Interfaces 7 (2015) 11824–11832.
[27] S. Barbosa, A. Topete, M. Alatorre-Meda, E.M. Villar-Alvarez, A. Pardo, C. Alvarez-Lorenzo, et al., Targeted combinatorial therapy using gold nanostars as theranostic platforms, J. Phys. Chem. C 118 (2014) 26313–26323.
[28] R. Grinyte, L. Saa, G. Garai-Ibabe, V. Pavlov, Biocatalytic etching of semiconductor cadmium sulfide nanoparticles as a new platform for the optical detection of analytes, Chem. Commun. 51 (2015) 17152–17155.
[29] M.N. Hoque, G. Das, Cationic tripodal receptor assisted formation of anion and anion–water clusters: structural interpretation of dihydrogen phosphate cluster and sulfate–water tetramer [(SO4)2–(H2O)2]4–, Cryst. Growth Des. 14 (2014) 2962–2971.
[30] Z. Chen, N. Zhang, Y.-J. Xu, Synthesis of graphene-ZnO nanorod nanocomposites with improved photoactivity and anti-photocorrosion, CrystEngComm 15 (2013) 3022–3030.
[31] J. Jin, J. Yu, G. Liu, P.K. Wong, Single crystal CdS nanowires with high visible-light photocatalytic H2-production performance, J. Mater. Chem. A 1 (2013) 10927–10934.
[32] M. Li, Y. Hu, S. Xie, Y. Huang, Y. Tong, X. Lu, Heterostructured ZnO/SnO2-x nanoparticles for efficient photocatalytic hydrogen production, Chem. Commun. 50 (2014) 4341–4343.
[33] J. Tang, Y. Wang, J. Li, P. Da, J. Geng, G. Zheng, Sensitive enzymatic glucose detection by TiO2 nanowire photoelectrochemical biosensors, J. Mater. Chem. A 2 (2014) 6153–6157.
[34] N. Sabir, N. Khan, J. Völkner, F. Widdascheck, P. del Pino, G. Witte, et al., Photo-electrochemical bioanalysis of guanosine monophosphate using coupled enzymatic reactions at a CdS/ZnS quantum dot electrode, Small 11 (2015) 5844–5850.
[35] J. Tian, Q. Liu, A.M. Asiri, A.H. Qusti, A.O. Al-Youbi, X. Sun, Ultrathin graphitic carbon nitride nanosheets: a novel peroxidase mimetic, Fe doping-mediated catalytic performance enhancement and application to rapid, highly sensitive optical detection of glucose, Nanoscale 5 (2013) 11604–11609.
[36] J. Li, X. Hong, D. Li, K. Zhao, L. Wang, H. Wang, et al., Mixed ligand system of cysteine and thioglycolic acid assisting in the synthesis of highly luminescent water-soluble CdTe nanorods, Chem. Commun. (2004) 1740–1741.
[37] Y. Dong, H. Zhang, Z.U. Rahman, L. Su, X. Chen, J. Hu, et al., Graphene oxide-Fe3O4 magnetic nanocomposites with peroxidase-like activity for colorimetric detection of glucose, Nanoscale 4 (2012) 3969–3976.
[38] W. Wei, Z. Wang, Z. Liu, Y. Liu, L. He, D. Chen, et al., Metal oxide hollow nanostructures: fabrication and Li storage performance, J. Power Sources 238 (2013) 376–387.

[39] H. Wang, Q. Liang, W. Wang, Y. An, J. Li, L. Guo, Preparation of flower-like SnO_2 nanostructures and their applications in gas-sensing and lithium storage, Cryst. Growth Design 11 (2011) 2942–2947.

Biographies

Yan Zhao received the M.S. degree in Analytical Chemistry from Qufu Normal University in 2016, now she is a Ph.D. candidate in the College of Chemistry and Chemical Engineering at Hunan University.

Jian Gong received her B.S. degree in 1989 from Department of Biology of Shandong Normal University and received her M.S. degree in 2004 from College of Life Science of Shandong Normal University. Currently, she is the president of Department of Pharmacy and Biotechnology of Zibo Vocational Institute.

Xiaobin Zhang received his B.S. degree in 2014 from Qufu Normal University. He is now an undergraduate in Qufu Normal University. His research mainly focuses on biosensor development and the application of tumor biomarker detection.

Dr. Rong-Mei Kong received her PhD (2011) in Analytical Chemistry in the Department of Chemistry at Hunan University. Currently, she is a lecturer in the College of Chemistry and Chemical Engineering at Qufu Normal University. Her research interests include constructing novel functional nucleic acids conjugated-nanostructures for bioassay and biosensor development.

Prof. Fengli Qu obtained her Ph.D. in analytical chemistry in Hunan University (China) in 2008. She worked in CPME-CNRS (Nancy, France) as a postdoctoral fellow from 2008 to 2009 and as a Visiting Professor in Princeton University (Princeton, USA) from 2013 to 2014. Currently, she is a Professor in the College of Chemistry and Chemical Engineering at Qufu Normal University. Her research interests include nanomaterial applications and biosensor development.